Histological evaluation of tendon formation using a scaffold-free three-dimensional-bioprinted construct of human dermal fibroblasts under in vitro static tensile culture

中西, 芳応

https://doi.org/10.15017/2348707

出版情報：Kyushu University, 2019, 博士（医学）, 課程博士
バージョン：
権利関係：

Regenerative Therapy 11 (2019) 47–55

Contents lists available at ScienceDirect

Regenerative Therapy

journal homepage: http://www.elsevier.com/locate/reth

Original Article

Histological evaluation of tendon formation using a scaffold-free three-dimensional-bioprinted construct of human dermal fibroblasts under *in vitro* static tensile culture

Yoshitaka Nakanishi [a], Takamitsu Okada [a, *], Naohide Takeuchi [a], Naoya Kozono [a], Takahiro Senju [a], Koichi Nakayama [b], Yasuharu Nakashima [a]

[a] Department of Orthopaedic Surgery, School of Medicine, Kyushu University, 3-1-1, Maidashi, Higashiku, Fukuoka-shi, Fukuoka, 812-8582, Japan
[b] Department of Regenerative Medicine and Biomedical Engineering, Faculty of Medicine, Saga University, Honjyo 1-chome, Honjyo-cho, Saga, 840-8502, Japan

ARTICLE INFO

Article history:
Received 6 December 2018
Received in revised form
11 January 2019
Accepted 3 February 2019

Keywords:
Tendon formation
In vitro study
Scaffold-free
Multicellular spheroid
Tensile culture
Human dermal fibroblast

ABSTRACT

Introduction: Tendon tissue engineering requires scaffold-free techniques for safe and long-term clinical applications and to explore alternative cell sources to tenocytes. Therefore, we histologically assessed tendon formation in a scaffold-free Bio-three-dimensional (3D) construct developed from normal human dermal fibroblasts (NHDFs) using our Bio-3D printer system under tensile culture *in vitro*.
Methods: Scaffold-free ring-like tissues were constructed from 120 multicellular spheroids comprising NHDFs using a bio-3D printer. Ring-like tissues were cultured *in vitro* under static tensile-loading with or without in-house tensile devices (tension-loaded and tension-free groups), with increases in tensile strength applied weekly to the tensile-loaded group. After a 4 or 8-week culture on the device, we evaluated histological findings according to tendon-maturing score and immunohistological findings of the middle portion of the tissues for both groups ($n = 4$, respectively).
Results: Histology of the tension-loaded group revealed longitudinally aligned collagen fibers with increased collagen deposition and spindle-shaped cells with prolonged culture. By contrast, the tension-free group showed no organized cell arrangement or collagen fiber structure. Additionally, the tension-loaded group showed a significantly improved tendon-maturing score as compared with that for the tension-free group at week 8. Moreover, immunohistochemistry revealed tenascin C distribution with a parallel arrangement in the tensile-loading direction at week 8 in the tension-loaded group, which exhibited stronger scleraxis-staining intensity than that observed in the tension-free group at weeks 4 and 8.
Conclusions: The NHDF-generated scaffold-free Bio-3D construct underwent remodeling and formed tendon-like structures under tensile culture *in vitro*.

1. Introduction

Tendon injury occurs under acute traumatic or chronic degenerative conditions and is very common [1–4]. Treatment of tendon injury often requires surgery to restore tendon function; however, for significant tendon loss in the extremities, which cannot be repaired by suturing, treatment options remain poorly defined. Although several methods using autografts or allografts have been reported, risks of damage to the donor site from which the autografts are harvested and potential immune reactions with allografts are major concerns [5–7].

Abbreviations: ESCs, embryonic stem cells; TDSCs, tendon-derived stem cells; 3D, three-dimensional; MCSs, multicellular spheroids; HDF, human dermal fibroblast; NHDFs, normal HDFs; H&E, hematoxylin and eosin; ECM, extracellular matrix; TGF, transforming growth factor.

* Corresponding author. Fax: +81 92 642 5507.
E-mail address: t-okada@ortho.med.kyushu-u.ac.jp (T. Okada).

Peer review under responsibility of the Japanese Society for Regenerative Medicine.

https://doi.org/10.1016/j.reth.2019.02.002

Engineering of tendon tissue can address these issues, and recently, several methods have been developed to repair tendon defects. For engineering of tendon tissue, uniaxial tensile culture is considered a key element, as it mimics the physiological conditions of tendons *in vivo* and allows cellular proliferation, differentiation, and matrix production [8]. Most previously reported methods used synthetic or biological scaffolds to form three-dimensional (3D) constructs and withstand the tensile force [8]. Cells adhere to the scaffolds, and the cell-scaffold construct is cultured under uniaxial mechanical loading to form tendon-like structures. However, the scaffolding materials can influence the surrounding microenvironment [9] or cause immunological reactions [10,11] in clinical settings.

It is critical to identify the appropriate cell source for tendon engineering [12]. For engineering tendon tissues, it is logical to use tenocytes as the cell source, because they are native cell types of intact tendon tissues. However, tenocytes exhibit limited proliferation and phenotype drift, and function loss has been observed during several passages *in vitro* [13]. Furthermore, the donor site is greatly limited, with donor-site morbidity reported after harvesting tendon tissue [14]. Therefore, several studies report alternative cell sources to tenocytes for tendon regeneration [12].

Previous studies demonstrated the possibility of tendon regeneration using scaffold-free cell sheets with human embryonic stem cells (ESCs) [15], rat tendon-derived stem cells (TDSCs) [16], and mouse dermal fibroblasts [17]. However, ESCs and TDSCs are multipotent, and considerable research needs to be conducted before they can be safely used for clinical applications [12,18]. By contrast, dermal fibroblasts are terminally differentiated cells and an easily accessible cell source in the absence of major donor-site morbidity for clinical applications [12,19]. Furthermore, previous studies using human dermal fibroblasts (HDFs) showed their high potential for tendon formation *in vitro* [12] and tendon regeneration *in vivo* [18]. However, tendon regeneration or formation using the scaffold-free method and HDFs has not been demonstrated.

In this study, we demonstrated tendon formation using a scaffold-free technique and HDFs *in vitro*. This technique involved tendon formation using a Bio-3D printer system developed by one of the coauthors (K.N.) and enabling the creation of robotically predesigned 3D structures using multicellular spheroids (MCSs) [20,21]. This system has been used for various tissue-regeneration applications, including for cartilage and subchondral bone [22], the aortae [23], peripheral nerves [24], the liver [25], the diaphragm [26], and the trachea [27].

Tis study assessed the possibility of achieving tendon formation using normal HDFs (NHDFs) and our novel scaffold-free technique *in vitro*. To do this, we engineered scaffold-free Bio-3D constructs with NHDFs using the Bio-3D printer system, cultured the constructs under tensile loading *in vitro*, and performed histologic evaluations.

2. Materials and methods

2.1. Cell culture

NHDFs (CC-2511; Lonza, Basel, Switzerland) were purchased and cultured in Dulbecco's modified Eagle medium (DMEM; Gibco, Grand island, NY, USA) containing 10% fetal bovine serum (Sigma–Aldrich, St. Louis, MO, USA), penicillin (100 U/mL), streptomycin (100 mg/mL), and ascorbic acid (50 μg/mL) at 37 °C in a humidified atmosphere of 5% CO_2. The culture medium was changed every 2–3 days, and cells were passaged to the same density (3500 cell/cm^2) until passage five, after which they were cryopreserved until further use.

2.2. Spheroid formation

The previously cryopreserved cells were thawed, plated on 150-mm culture dishes (3500 cells/cm^2), and cultured in the same medium until 90% confluence. The cells (passage 6) were detached by recombinant trypsin replacement, resuspended in the same medium without ascorbic acid, and seeded into 96-well plates designed to prevent cells from adhering to the culture-plate surface (Sumilon PrimeSurface; Sumitomo Bakelite, Tokyo, Japan) at 2.5×10^4 cells/well. After incubation for 36 h, the cells spontaneously aggregated into MCSs (Fig. 1a).

2.3. The Bio-3D printer for generating NHDF ring tissue

We used a Bio-3D printer (Regenova; Cyfuse, Tokyo, Japan) to assemble MCSs for constructing scaffold-free ring-like tissues, as described by Ito et al. [23]. Briefly, a ring-like structure was predesigned by arranging 120 spheroids in two layers, nine horizontally and 20 vertically, on the computer system (Fig. 1b.). According to the predesiged 3D structure, the printer device (Fig. 1c.) robotically selected MCSs with a diameter of 500 μm–600 μm and skewered them individually into a 9×9 needle-array similar to a "Kenzan" (Fig. 1d). The medium used for the culture of constructs on the needle array was the same as that used for the cell culture. After 8 days, adjacent spheroids were fused to form a ring-like shape in the Kenzan, which was then removed (Fig. 1e).

2.4. Tensile culture of tissue

The ring-like tissues developed from the NHDFs were cultured under static mechanical strain that was generated using a self-made, in-house device with stainless steel springs (Fig. 1f). The device comprised three bases (main, middle, and spring-anchor bases) (Fig. 1f and g), with the middle and spring-anchor bases situated on the main base in order to allow their smooth movement. The three bases were connected using four springs, and pinholes were created on the floor of the main base at 1-mm intervals. Upon generating tensile force to the tissues, the spring-anchor base was moved to the right side, and a stainless pin was inserted into a hole in the main base between the middle base and the spring-anchor base.

The spring-anchor base was then immobilized by the elastic force of the springs and the stainless-steel pin, and the middle base was moved to the right side, where it stopped at the balance point of the springs (Fig. 1f). In the tension-loaded group, the four ring-like tissues were placed on the main and middle bases, and tensile force on the tissues was generated using the previously described mechanism (Fig. 1g and i). This device can adjust the traction force by changing the spring constant and moving distance of the fixed base. In this study, we used stainless steel springs (Riken Spring Industry, Osaka, Japan) with an extremely low spring constant ($K = 4.4 \times 10^{-4}$ N/mm).

The initial force was determined at the initial point, which was the distance between the main and middle bases and lower with the tissues than it was in their absence (Fig. 1g.). Furthermore, the spring-anchor base was moved 2 mm to the right side weekly in order to maintain the traction force because of tissue elongation. The tissues were cultured with the same growth medium under the same cell-culture conditions, and the culture medium was changed twice weekly. The tension-free tissues were placed in the same device and cultured using the same protocol without moving the spring-anchor base (Fig. 1h).

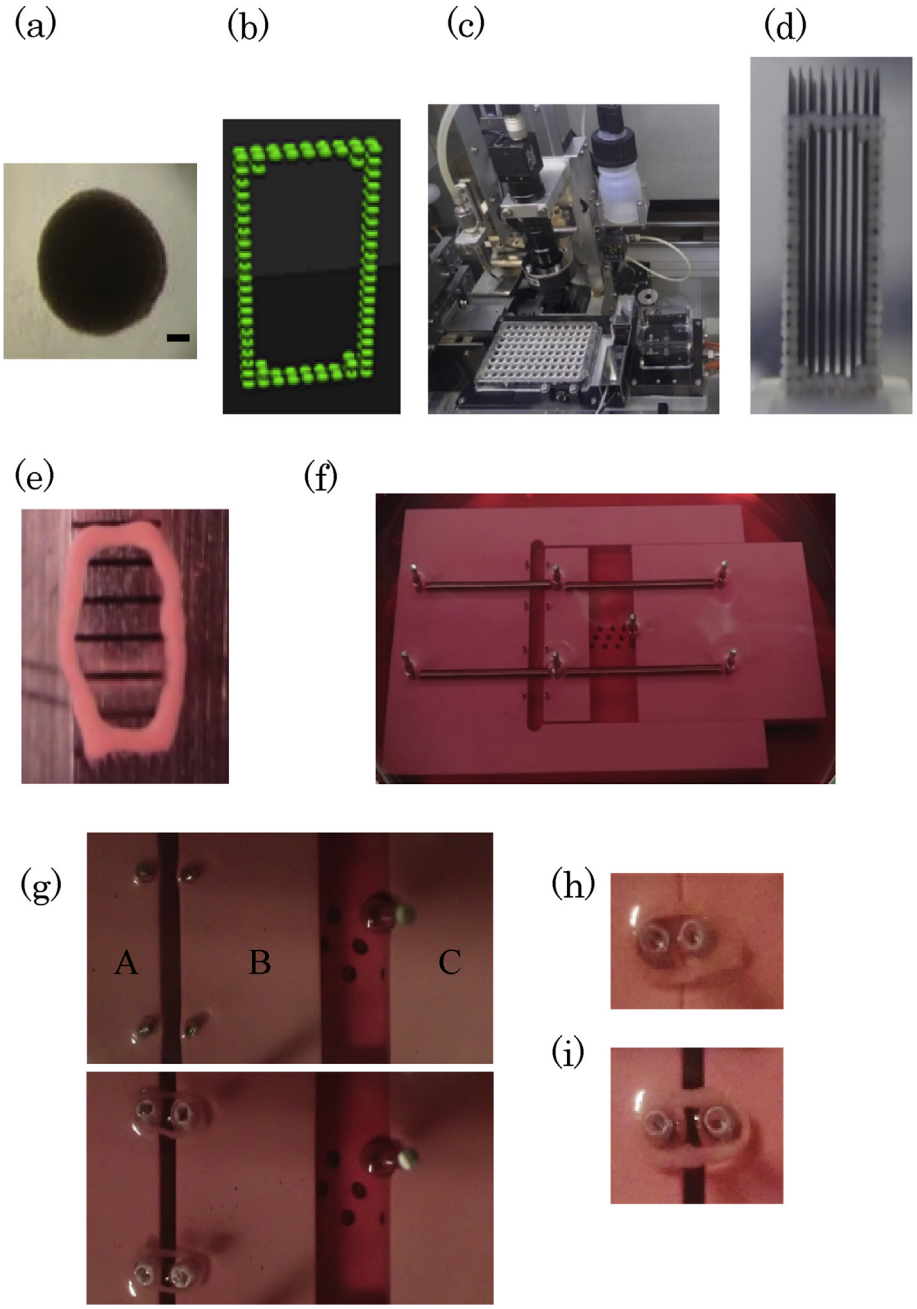

Fig. 1. Materials for and process of manufacturing three-dimensional (3D) Bio-printed ring-like tissue and human neo-tendon tissue under static tensile loading. (a) Image of multicellular spheroid (MCS) produced from normal human dermal fibroblasts (NHDFs). Scale bar = 100 μm. (b) Predesigned 3D ring-like structure. Green spheres represent MCSs. (c) Image of the Bio-3D printer (Regenova). (d) Image of the Kenzan needle-array after skewering MCSs. (e) Image of ring-like tissue after removal from the needle array. (f) Image of the in-house uniaxial tensile device. (g) Image of the tensile device without tissues (upper) and with tissues (lower) at the initial strength point. A: main, B: middle, and C: spring-anchor base. Image of ring-like tissues in the (h) tension-free and (i) tension-loaded groups.

2.5. Histology

After a 4- or 8-week culture on the tensile device, we harvested the tissues from the tensile device for both groups. All tissues were immediately fixed in 4% paraformaldehyde, followed by three washes in phosphate-buffered saline, dehydrated with alcohol and xylene, and embedded in paraffin blocks. Histological sections (7 μm) were prepared using a microtome and subsequently stained with hematoxylin and eosin (H&E) and Masson trichrome. H&E staining was used to examine the tissue structure, nuclear morphology, and cell distribution. Trichrome staining revealed collagen production, collagen-fiber direction, and the proportion of fibers oriented in parallel.

2.6. Evaluation using tendon-maturing scoring

We evaluated the maturation of the scaffold-free Bio-3D cell construct using the tendon-maturing scoring system described by Watkins et al. [28] and modified by Ide et al. [29]. Assessment of vascularity and tendon-to-bone insertion was excluded, because

these parameters were not associated with this *in vitro* study, whereas the remaining five parameters (cellularity, proportion of cells resembling tenocytes, proportion of parallel cells, proportion of fibers of large diameter characteristic of mature tendon fibers, and proportion of parallel fibers) were semiquantitatively assessed (Table 1). Cellularity, the proportion of cells resembling tenocytes, and proportion of cells oriented in parallel were assessed using H&E staining while the other parameters were assessed using trichrome staining.

These parameters were semiquantitatively graded using a four-point scale (I–IV; Table 1). Cellularity was graded as marked (grade I), moderate (grade II), mild (grade III), and minimal (grade IV). Other parameters were graded as <25% of proportion (grade I), 25%–50% of proportion (grade II), 50%–75% of proportion (grade III), and >75% of proportion (grade IV). Based on this assessment, a maximum score was 20, which would be that for a normal tendon. The same length was evaluated from the center of the tissues for both groups using the histological score. Cross-sections were examined under a microscope (AX70; Olympus, Tokyo, Japan) and analyzed using Image J software (version 1.46c; National Institutes of Health, Bethesda, MD, USA). Scoring was performed by two blinded colleagues with no information about the data, including the application of traction or non-traction and the incubation period of the culture. In cases of disagreement, the findings were reviewed by the observers and discussed until reaching agreement.

2.7. Immunohistochemistry

Immunohistochemistry was performed using rabbit anti-human tenascin C monoclonal (ab108930; Abcam, Cambridge, UK) or rabbit anti-human scleraxis polyclonal (ab58655; Abcam) antibodies. Tissue sections on slides were deparaffinized, incubated with methanol and 0.3% hydrogen peroxide (H_2O_2) for 30 min, and washed. The slides were then incubated with the respective primary antibodies (1:200) at 4 °C overnight. After additional washing steps, the slides were further incubated with horseradish-conjugated secondary polyclonal rabbit immunoglobulin G antibodies (ImmPRESS reagent anti-rabbit Ig kit; Vector Laboratories Burlingame, CA, USA). After additional washing steps, immunoreactivity was visualized using a diaminobenzidine peroxidase substrate kit (Vector Laboratories), followed by counterstaining with hematoxylin. Negative controls were samples immunostained without the primary antibody.

2.8. Statistical analyses

Statistical analyses were performed using JMP software (v13.0.0; SAS Institute, Inc., Cary, NC, USA). P-values were calculated for differences in the tendon-maturing score using one-way analysis of variance with a Tukey–Kramer post hoc test. Differences were considered significant at $P < 0.05$. All data are presented as the mean ± standard deviation.

3. Results

3.1. Gross and histological findings

In both groups, the bilateral middle portion of the ring-like tissues gradually closed and fused following prolonged culture (Figs. 2a and 3a), and tissues completely changed form to a glass-like shape by week 4 (Figs. 2b and 3b). In the tension-loaded group up to week 2, the tissue was contracted despite the tensile force being increased weekly. From week 2–6, the tissue elongated as the tensile force increased; however, after week 6, the tissue length had not elongated despite the increased tensile strength. By contrast, the tissues contracted in the tension-free group with prolonged culture (Fig. 2a–c). Therefore, the shape of the fused middle portion differed between the two groups, with the tension-loaded group narrower and longer than the tension-free group was (Figs. 2b and c, 3b and c).

We then histologically evaluated the fused central portion of both groups having the same length. At week 4, H&E staining of tissue from both groups revealed few cells with elongated nuclei similar to tenocytes, and the cell arrangement lacked organization (Figs. 2d and 3d). Additionally, trichrome staining revealed collagen deposition with a disorganized fiber direction (Figs. 2e and f, 3e and f).

In the tension-free group at week 8, H&E staining revealed that the tissues were less cellular than those at week 4 (Fig. 2g); however, staining revealed no visible disruption of the organized cell arrangement and an increase in cells with elongated nuclei. Moreover, trichrome staining revealed no noticeable increase in collagen deposition and disruption of collagen fiber arrangement (Fig. 2h and i). Conversely, in the tension-loaded group at week 8, H&E staining showed longitudinally aligned cells with elongated nuclei similar to tenocytes along with collagen fibers (Fig. 3g). Additionally, trichrome staining revealed significant collagen deposition with an organized fiber direction (Fig. 3h and i). Surprisingly, it also revealed a wave structure that mimicked native tendon tissue (Fig. 3h and i).

The tendon-maturing scores of the tension-free and -loaded groups at week 4 were 5.25 ± 0.43 and 7.00 ± 0.71, respectively, and at week 8, the scores were 7 ± 1.22 and 13.75 ± 1.48, respectively. Table 2 summarizes of the scores of all evaluated items. The tension-loaded group had a significantly higher score at week 8 relative to week 4 ($P < 0.0001$) and higher than that for the tension-free group at weeks 4 and 8 (both $P < 0.0001$; Fig. 4).

3.2. Production of tenascin C

Immunohistochemical analysis revealed tenascin C production after 4 and 8 weeks of culture in both groups (Fig. 5.). In both groups at week 4, the tenascin C distribution was unorganized (Fig. 5a,c,f and h), with the tension-free group showing similar patterns at week 8 (Fig. 5b and g). By contrast, in the tension-loaded group at week 8, the tenascin C distribution was arranged parallel to the direction of tensile loading (Fig. 5d and i).

Table 1
Modified tendon-maturing score.

	1	2	3	4
Cellularity	Marked	Moderate	Mild	Minimal
Proportion of cells resembling tenocytes	<25%	25–50%	50–75%	>75%
Proportion of cells oriented in parallel	<25%	25–50%	50–75%	>75%
Proportion of fibers of large diameter characteristic of mature tendon fibers	<25%	25–50%	50–75%	>75%
Proportion of fibers oriented in parallel	<25%	25–50%	50–75%	>75%

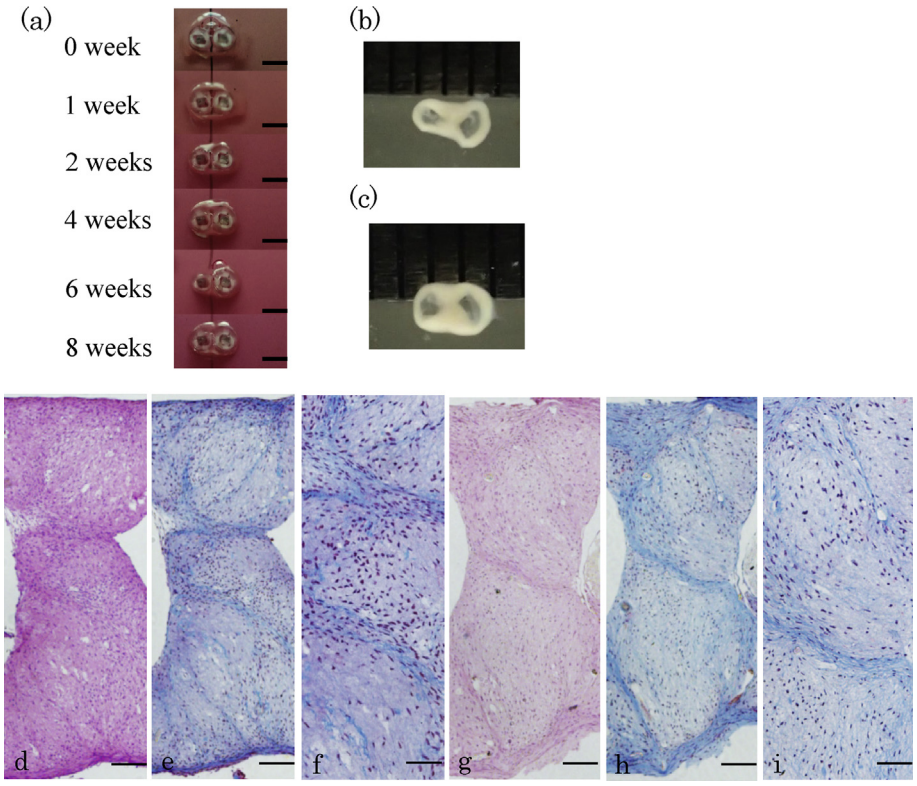

Fig. 2. Histological analysis of the tension-free group. Images showing changes in construct shape with prolonged culture (a) and gross view at weeks 4 (b) and 8 (c). Photomicrographs showing hematoxylin and eosin (H&E) staining (d and g) and Masson's trichrome staining (e, f, h, and i) of *in vitro*-cultured tissue without tension-loading at weeks 4 (b and d–f) and 8 (c and g–i). Scale bars = 2 mm (a), 100 μm (d, e, h, and i), and 50 μm (f and i).

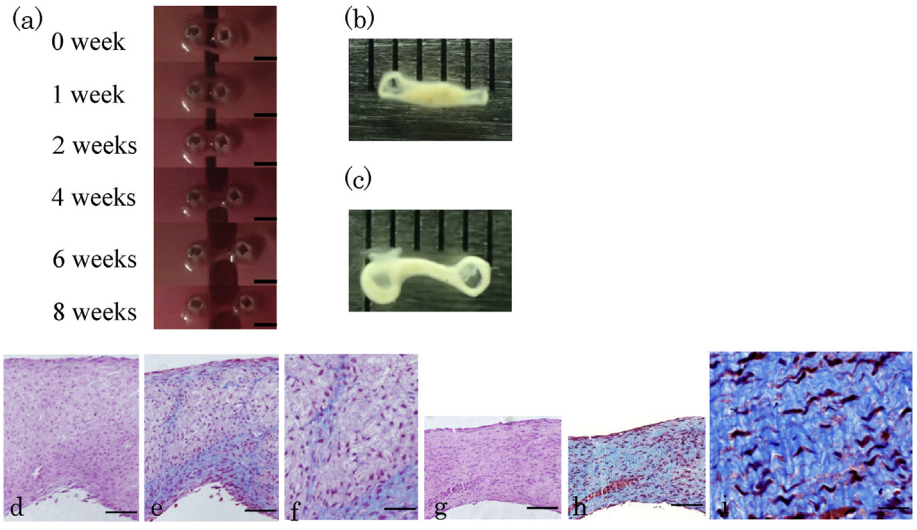

Fig. 3. Histological analysis of the tension-loaded group. Images showing changes in construct shape with prolonged culture (a) and gross view at weeks 4 (b) and 8 (c). Photomicrographs showing hematoxylin and eosin (H&E) staining (d and g) and Masson's trichrome staining (e, f, h, and i) of *in vitro*-cultured tissue with tension loading at weeks 4 (b and d–f) and 8 (c and g–i). Scale bars = 2 mm (a), 100 μm (d, e, g, and h), 50 μm (f) and 20 μm (i).

3.3. *Expression of scleraxis*

At week 4, immunohistochemical analysis revealed that scleraxis expression was stronger in the tension-loaded group than it was in the tension-free group (Fig. 6 a, c, f, and h). At week 8, the tension-loaded group maintained scleraxis-staining intensity relative to that at week 4, which was also stronger than that in the tension-free group (Fig. 6b,d,i and g).

4. Discussion

Our results demonstrated that tendon formation was possible using NHDFs and our novel scaffold-free technique *in vitro*. Although a previous study reported tendon regeneration with scaffold-free techniques using mouse dermal fibroblasts [17], to the best of our knowledge, this is the first report of tendon regeneration or formation using a scaffold-free technique and HDFs.

Table 2
Histological analysis.

	Tension-free group				Tension-loaded group			
	1	2	3	4	1	2	3	4
Week 4 evaluation, *n*								
Cellularity	4	0	0	0	1	3	0	0
Fibrocytes	4	0	0	0	4	0	0	0
Fiber diameter	4	0	0	0	1	3	0	0
Cells, parallel	4	0	0	0	3	1	0	0
Fibers, parallel	3	1	0	0	3	1	0	0
Week 8 evaluation, *n*								
Cellularity	1	3	0	0	0	4	0	0
Fibrocytes	4	0	0	0	0	3	1	0
Fiber diameter	2	2	0	0	0	1	1	2
Cells, parallel	4	0	0	0	0	3	1	0
Fibers, parallel	1	3	0	0	0	0	0	4

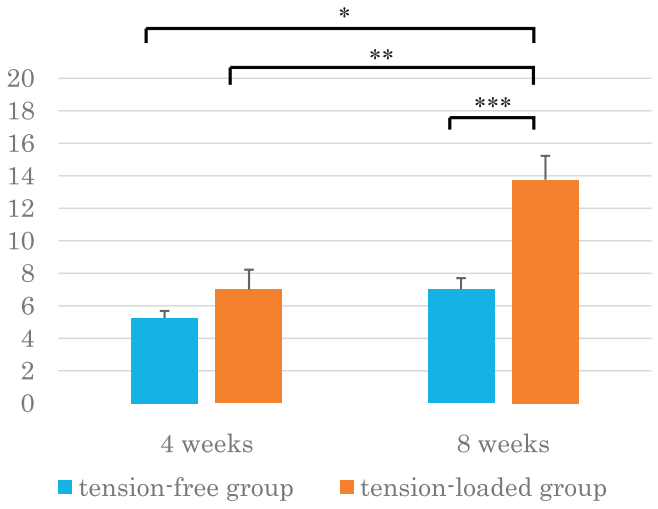

Fig. 4. Histological scoring. Histological scoring of tension-free and tension-loaded groups at weeks 4 and 8. A perfect score on this scale is 20 points. *P < 0.0001; **P < 0.0001; and ***P < 0.0001 ($n = 4$).

examination showed an increase in the proportion of elongated nucleated cells, parallel collagen fibers, and elongated cells in the loading direction along with a waveform structure, although the cellularity remained moderate. Native tendons comprise cells and ECM, which are largely composed of collagen fibrils [30]. Collagen-fiber bundles form parallel and waveform structures, with interposed, elongated, parallel tenocytes. In this study, the tension-loaded group showed these tendon-specific histological features and mimicked native tendons.

Furthermore, immunohistochemical analysis showed that the tension-loaded group produced tenascin C, which was distributed in a parallel arrangement to the direction of tensile loading. By contrast, although the tension-free group also showed tenascin C production, the distribution lacked organization. Tenascin C is a glycoprotein constituent of the tendon ECM and is distributed on the cell–collagen fiber interface and the surface of collagen-fiber bundles in native tendons [31]. Conversely, tenascin C is rarely detected in the healthy dermis [32], which is the source for NHDFs; therefore we evaluated tenascin C expression as a marker of tendon formation using NHDFs. Chen et al. [33] reported that a rabbit dermal fibroblast cell-scaffold construct transplanted into a defective rabbit Achilles tendon produced tenascin C in a parallel arrangement with collagen fiber. In the present study, the distribution pattern of tenascin C in the tension-loading group was similar to that reported previously.

Additionally, immunohistochemical analysis showed overexpression of scleraxis in the tension-loaded group. Scleraxis directly regulates the transcription of type 1 collagen, which is the main component of the tendon ECM [34]. Scleraxis is predominantly expressed by tendon progenitors and differentiated tendon cells [35], whereas previous studies showed a lack of scleraxis expression on dermal fibroblasts cultured *in vitro* [18,36]. Moreover, scleraxis-knockout mice displayed a less organized and reduced tendon ECM [37], and scleraxis was identified as a critical factor in tendon development and differentiation [38]. In the present study, the tension-free group showed a lack of scleraxis expression and formed immature tissue as compared with the tension-loaded group. Our results suggested that scleraxis over-

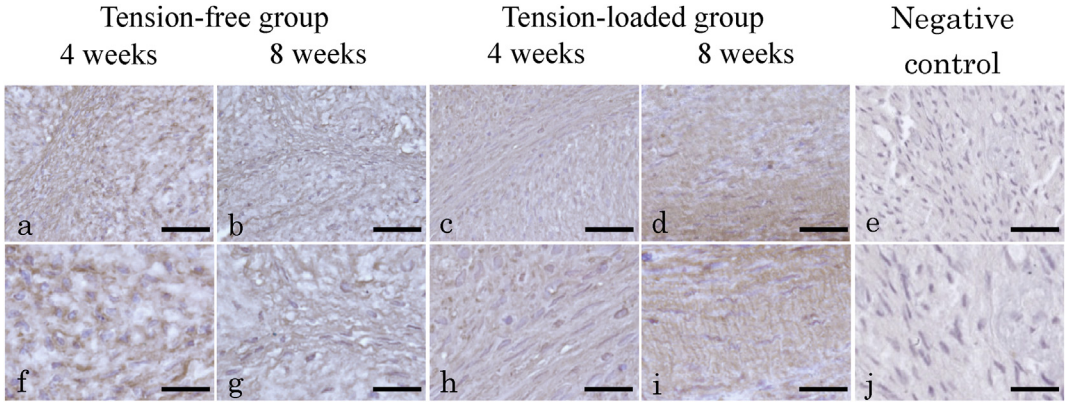

Fig. 5. Immunohistochemical analysis of tenascin. Photomicrographs of immunohistochemical staining for tenascin C (a–d) and the magnification (f–i). (e and j) Negative controls for immunostaining. Scale bars = 50 μm (a–e) and 20 μm (f–j).

Furthermore, this is the first report of tendon regeneration or formation using a scaffold-free Bio-3D printer system. Despite the absence of a biological scaffold, our scaffold-free NHDF cell constructs exhibited elasticity and could be cultured with tensile loading using an in-house tensile device. Furthermore, histological expression was vital for the formation of tendon-like tissue using NHDFs with our method.

Unlike the tension-free group, the tension-loaded group showed scleraxis overexpression and formed tendon-like tissue with an organized distribution of collagen fiber and tenascin C. Our results

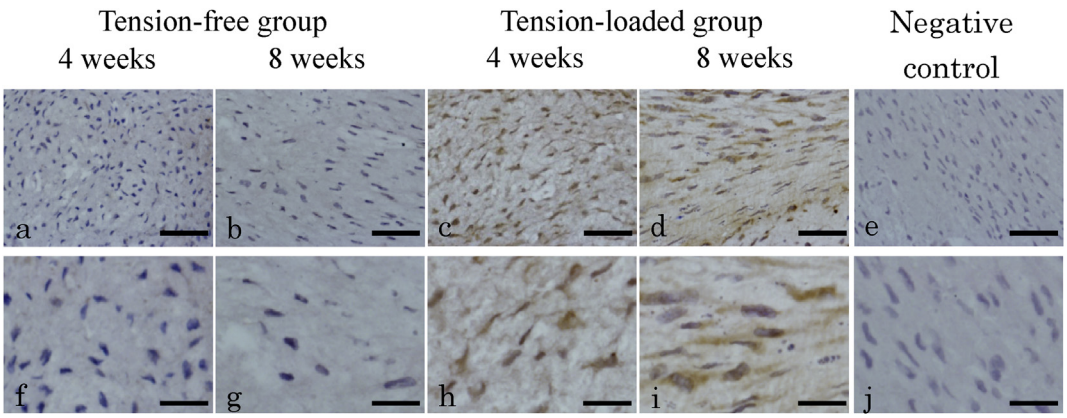

Fig. 6. Immunohistochemical analysis of scleraxis. Photomicrographs of immunohistochemical staining for scleraxis (a–d) and the magnification (f–i). (e and j) Negative controls for immunostaining. Scale bars = 50 μm (a–e) and 10 μm (f–j).

indicated that mechanical loading is a key element for the formation of tendon-like tissue using NHDFs with our method. Dermal fibroblasts synthesize dermis ECM proteins, which mainly comprise type I collagen fibrils [39] similar to native tendon tissue [34]. Mechanical loading reportedly induces collagen synthesis and the production of growth factors, such as transforming growth factor (TGF)-β1, by cultured dermal fibroblasts [40]. Additionally, Wang et al. [41] reported that exogenous TGF-β1 enhances scleraxis expression in cultured dermal fibroblasts. These findings suggest that HDFs might have upregulated scleraxis expression in response to mechanical stress.

In the tension-loaded group, the ring-like Bio-3D construct contracted until week 2 and elongated thereafter. A previous report reported that tissue without fixation at both ends gradually contracted with prolonged culture [12]. Up to week 2, the tensile force might have been too weak to maintain the length of the ring-like tissue; however, the tissue length did not clearly elongate after week 6 despite the tensile strength being increased weekly. Our results showed that the tendon-maturing score at week 8 was significantly higher than that at week 4 in the tension-loaded group. Therefore, the maturation of tendon-like structure on the tissue might have enabled resistance to the traction force and maintained the tissue length.

Scaffold-free methods for tissue engineering avoid problems associated with the use of scaffold biomaterials, including immunogenicity, biomaterial degradation, and the toxicity of degradation products [42]. Therefore, our method and previous scaffold-free methods using cell sheets [15–17] can be considered highly safe for tendon regeneration or formation for clinical application. Our method differs from previous methods using cell sheets for forming scaffold-free Bio-3D cell constructs, as the scaffold-free cell constructs are formed using a Bio-3D printer system that forms constructs of various shapes and sizes by changing the predesigned 3D structure using a computer system and an appropriate Kenzan design [22,23,26,43]. In the present study, we used a standard sized Kenzan-like needle array to engineer the Bio-3D constructs, and our tendon-like tissue was small in size. It is possible that using a longed Kenzan-like needle array [26] might enable the formation of larger tendon-like tissue.

To form tendon-like tissue, we engineered a ring-like Bio-3D construct with our Bio-3D printer system. In order to culture the Bio-3D construct with tensile loading, it was necessary to fix both ends of the tissue. In the method using scaffolds, crumping both ends is often used [44]; however, our immature construct was fragile, making it difficult to apply tensile loading with crump fixation. Therefore, we addressed this problem by forming it into a ring shape.

Additionally, we used a static tensile device with stainless steel springs. For engineering tendon-like tissue, previous methods used cyclic tensile loading with a bioreactor system in order to mimic the physiological nature of mechanical loading for the tendon tissue [8]. For cyclic tensile loading, it is important to adjust the strain amplitude in order to adapt the construct [45]. In the present study, it was difficult to maintain constant strain amplitude due to tissue elongation. By contrast, a previous report described engineering tendon-like tissue with HDFs on a static tensile culture using stainless steel springs [12]. Therefore, we modified their method to create a tensile device using stainless steel springs in order to adapt to our ring-like Bio-3D construct. We used stainless steel springs with an extremely low spring constant in order to not break the Bio-3D construct with the tensile force and increased the tensile strength weekly as the tissue maturated during culture.

Our study has some limitations. First, we did not elucidate the similarities and differences between our tendon-like tissues generated using NHDFs and normal tendon tissues in detail. One of the reasons is the lack of specific tendon markers, which are only expressed in normal tendon tissues [46]. Second, the tension-loading group at week 8 showed less maturity than normal tendon tissue according to the tendon-maturing score. Given that bacterial contamination occurs during prolonged culture, further study is needed to explore an ideal culture method, including a traction protocol, which would enable the formation of mature tendon-like tissue in a short period of time. Additionally, we evaluated tendon formation by histological assessment alone. For clinical application, further study is needed to adjust the size of the tendon-like tissue and assess its functional aspects, including mechanical properties or performance, *in vivo* after transplantation into a tendon-defect animal model.

5. Conclusion

This study demonstrated tendon formation using a scaffold-free technique and NHDFs *in vitro*. We engineered scaffold-free Bio-3D cell constructs using our scaffold-free Bio-3D printer system with NHDFs and cultured them under tensile loading *in vitro*. The tension-loaded group at week 8 showed that the proportion of elongated nuclear cells and parallel cells in the tensile direction was higher than that at week 4. Furthermore, collagen fiber and tenascin C were distributed in an arrangement parallel to the direction of tensile loading, and we found that the dermal fibroblasts strongly expressed scleraxis to a degree similar as that observed at

week 4. These findings indicated that our scaffold-free method allowed tendon formation using HDFs *in vitro*.

Contributions

Y.N., T.O., N.T., and K.N. designed the study. Y.N. performed and analyzed all experiments and wrote the manuscript. T.S. and N.K. contributed to the experiments. T.O., N.T., and K.N. revised the manuscript. Y. N supervised the overall project.

Declaration of interests

K. Nakayama is a co-founder and shareholder of Cyfuse Biomedical KK and an investor/developer designated on the patent for the Bio-3D printer. Patent title: Method for Production of Three-Dimensional Structure of Cells; patent number: JP4517125. Patent title: Cell Structure Production Device; patent number: JP5896104.

Acknowledgments

We thank XY. Zhang, H. Kimura, and T. Tamura for their technical assistance. Additionally, we are grateful to Dr. Junji Kishimoto for his helpful contribution to the statistics. This work was supported by Grants-in-Aid for Scientific Research (16K10864) from the Japan Society for the Promotion of Science.

Appendix A. Supplementary data

Supplementary data to this article can be found online at https://doi.org/10.1016/j.reth.2019.02.002.

References

[1] Huang HH, Qureshi AA, Biundo JJ. Sports and other soft tissue injuries, tendinitis, bursitis, and occupation-related syndromes. Curr Opin Rheumatol 2000;12:150–4.
[2] Chen JM, Xu JK, Wang AL, Zheng MH. Scaffolds for tendon and ligament repair: review of the efficacy of commercial products. Expert Rev Med Devices 2009;6:61–73.
[3] Yamamoto A, Takagishi K, Osawa T, Yanagawa T, Nakajima D, Shitara H, et al. Prevalence and risk factors of a rotator cuff tear in the general population. J Shoulder Elbow Surg 2010;19:116–20.
[4] Clayton RAE, Court-Brown CM. The epidemiology of musculoskeletal tendinous and ligamentous injuries. Injury 2008;39:1338–44.
[5] Cerullo G, Puddu G, Gianní E, Damiani A, Pigozzi F. Anterior cruciate ligament patellar tendon reconstruction: it is probably better to leave the tendon defect open! Knee Surg Sports Traumatol Arthrosc 1995;3(1):14–7.
[6] Coupens SD, Yates CK, Sheldon C, Ward C. Magnetic-resonance-imaging evaluation of the patellar tendon after use of its central one-third for anterior cruciate ligament reconstruction. Am J Sports Med 1992;20:332–5.
[7] Harner CD, Olson E, Irrgang JJ, Silverstein S, Fu FH, Silbey M. Allograft versus autograft anterior cruciate ligament reconstruction: 3- to 5-year outcome. Clin Orthop Relat Res 1996:134–44.
[8] Wang T, Gardiner BS, Lin Z, Rubenson J, Kirk TB, Wang A, et al. Bioreactor design for tendon/ligament engineering. Tissue Eng B Rev 2013;19:133–46.
[9] Koga H, Muneta T, Ju YJ, Nagase T, Nimura A, Mochizuki T, et al. Synovial stem cells are regionally specified according to local microenvironments after implantation for cartilage regeneration. Stem Cell 2007;25:689–96.
[10] Anderson JM, Rodriguez A, Chang DT. Foreign body reaction to biomaterials. Semin Immunol 2008;20:86–100.
[11] Badylak SE, Gilbert TW. Immune response to biologic scaffold materials. Semin Immunol 2008;20:109–16.
[12] Deng D, Liu W, Xu F, Yang Y, Zhou GD, Zhang WJ, et al. Engineering human neo-tendon tissue in vitro with human dermal fibroblasts under static mechanical strain. Biomaterials 2009;30:6724–30.
[13] Yao L, Bestwick CS, Bestwick LA, Maffulli N, Aspden RM. Phenotypic drift in human tenocyte culture. Tissue Eng 2006;12:1843–9.
[14] Kartus J, Movin T, Karlsson J. Donor-site morbidity and anterior knee problems after anterior cruciate ligament reconstruction using autografts. Arthroscopy 2001;17:971–80.
[15] Chen X, Song XH, Yin Z, Zou XH, Wang LL, Hu H, et al. Stepwise differentiation of human embryonic stem cells promotes tendon regeneration by secreting fetal tendon matrix and differentiation factors. Stem Cell 2009;27:1276–87.
[16] Ni M, Rui YF, Tan Q, Liu Y, Xu LL, Chan KM, et al. Engineered scaffold-free tendon tissue produced by tendon-derived stem cells. Biomaterials 2013;34:2024–37.
[17] Tang QM, Chen JL, Shen WL, Yin Z, Liu HH, Fang Z, et al. Fetal and adult fibroblasts display intrinsic differences in tendon tissue engineering and regeneration. Sci Rep 2014 Jul 3;4:5515.
[18] Chen B, Ding J, Zhang W, Zhou G, Cao Y, Liu W, et al. Tissue engineering of tendons: a comparison of muscle-derived cells, tenocytes, and dermal fibroblasts as cell sources. Plast Reconstr Surg 2016;137. 536e-44e.
[19] Clarke AW, Alyas F, Morris T, Robertson CJ, Bell J, Connell DA. Skin-derived tenocyte-like cells for the treatment of patellar tendinopathy. Am J Sports Med 2011;39:614–23.
[20] Nakayama K. In vitro biofabrication of tissues and organs. Biofabrication 2013:1–21.
[21] Moldovan NI, Hibino N, Nakayama K. Principles of the kenzan method for robotic cell spheroid-based three-dimensional bioprinting. Tissue Eng B Rev 2017;23:237.
[22] Ishihara K, Nakayama K, Akieda S, Matsuda S, Iwamoto Y. Simultaneous regeneration of full-thickness cartilage and subchondral bone defects in vivo using a three-dimensional scaffold-free autologous construct derived from high-density bone marrow-derived mesenchymal stem cells. J Orthop Surg Res 2014;9.
[23] Itoh M, Nakayama K, Noguchi R, Kamohara K, Furukawa K, Uchihashi K, et al. Scaffold-Free Tubular Tissues Created by a Bio-3D Printer Undergo Remodeling and Endothelialization when Implanted in Rat Aortae. PLoS One 2015;10:10. e0136681, 2015.
[24] Yurie H, Ikeguchi R, Aoyama T, Kaizawa Y, Tajino J, Ito A, et al. The efficacy of a scaffold-free Bio 3D conduit developed from human fibroblasts on peripheral nerve regeneration in a rat sciatic nerve model. PLoS One 2017;12.
[25] Yanagi Y, Nakayama K, Taguchi T, Enosawa S, Tamura T, Yoshimaru K, et al. In vivo and ex vivo methods of growing a liver bud through tissue connection. Sci Rep UK 2017;7.
[26] Zhang XY, Yanagi Y, Sheng Z, Nagata K, Nakayama K, Taguchi T. Regeneration of diaphragm with bio-3D cellular patch. Biomaterials 2018;167:1–14.
[27] Taniguchi D, Matsumoto K, Tsuchiya T, Machino R, Takeoka Y, Elgalad A, et al. Scaffold-free trachea regeneration by tissue engineering with bio-3D printing. Interact Cardiov Th 2018;26:745–52.
[28] Watkins JP, Auer JA, Gay S, Morgan SJ. Healing of surgically created defects in the equine superficial digital flexor tendon - collagen-type transformation and tissue morphologic reorganization. Am J Vet Res 1985;46:2091–6.
[29] Ide J, Kikukawa K, Hirose J, Iyama K, Sakamoto H, Mizuta H. The effects of fibroblast growth factor-2 on rotator cuff reconstruction with acellular dermal matrix grafts. Arthroscopy 2009;25:608–16.
[30] Franchi M, Trirè A, Quaranta M, Orsini E, Ottani V. Collagen structure of tendon relates to function. ScientificWorldJournal 2007 Mar 30;7:404–20.
[31] Jarvinen TAH, Jozsa L, Kannus P, Jarvinen TLN, Hurme T, Kvist M, et al. Mechanical loading regulates the expression of tenascin-C in the myotendinous junction and tendon but does not induce de novo synthesis in the skeletal muscle. J Cell Sci 2003;116:857–66.
[32] Latijnhouwers M, Bergers M, Ponec M, Dijkman H, Andriessen M, Schalkwijk J. Human epidermal keratinocytes are a source of tenascin-C during wound healing. J Invest Dermatol 1997;108:776–83.
[33] Chen CH, Chen SH, Kuo CY, Li ML, Chen JP. Response of dermal fibroblasts to biochemical and physical cues in aligned polycaprolactone/silk fibroin nanofiber scaffolds for application in tendon tissue engineering. Nanomaterials 2017;vol. 7.
[34] Lejard V, Brideau G, Blais F, Salingcarnboriboon R, Wagner G, Roehrl MHA, et al. Scleraxis and NFATc regulate the expression of the pro-alpha 1(I) collagen gene in tendon fibroblasts. J Biol Chem 2007;282:17665–75.
[35] Schweitzer R, Chyung JH, Murtaugh LC, Brent AE, Rosen V, Olson EN, et al. Analysis of the tendon cell fate using Scleraxis, a specific marker for tendons and ligaments. Development 2001;128:3855–66.
[36] Naitoh M, Kubota H, Ikeda M, Tanaka T, Shirane H, Suzuki S, et al. Gene expression in human keloids is altered from dermal to chondrocytic and osteogenic lineage. Genes Cells 2005;10:1081–91.
[37] Murchison ND, Price BA, Conner DA, Keene DR, Olson EN, Tabin CJ, et al. Regulation of tendon differentiation by scleraxis distinguishes force-transmitting tendons from muscle-anchoring tendons. Development 2007;134:2697–708.
[38] Liu HH, Zhu SA, Zhang C, Lu P, Hu JJ, Yin Z, et al. Crucial transcription factors in tendon development and differentiation: their potential for tendon regeneration. Cell Tissue Res 2014;356:287–98.
[39] Xia W, Hammerberg C, Li Y, He T, Quan T, Voorhees JJ, et al. Expression of catalyticallssy active matrix metalloproteinase-1 in dermal fibroblasts induces collagen fragmentation and functional alterations that resemble aged human skin. Aging Cell 2013;12:661–71.
[40] Kuang R, Wang Z, Xu Q, Liu S, Zhang W. Influence of mechanical stimulation on human dermal fibroblasts derived from different body sites. Int J Clin Exp Med 2015;8:7641–7.
[41] Wang W, Li J, Wang K, Zhang Z, Zhang W, Zhou G, et al. Induction of predominant tenogenic phenotype in human dermal fibroblasts via synergistic effect of TGF-beta and elongated cell shape. Am J Physiol Cell Physiol 2016;310:C357–72.

[42] Williams DF. On the mechanisms of biocompatibility. Biomaterials 2008;29:2941–53.
[43] Noguchi R, Nakayama K, Itoh M, Kamohara K, Furukawa K, Oyama J, et al. Development of a three-dimensional pre-vascularized scaffold-free contractile cardiac patch for treating heart disease. J Heart Lung Transplant 2016;35:137–45.
[44] Qin TW, Sun YL, Thoreson AR, Steinmann SP, Amadio PC, An KN, et al. Effect of mechanical stimulation on bone marrow stromal cell-seeded tendon slice constructs: a potential engineered tendon patch for rotator cuff repair. Biomaterials 2015;51:43–50.
[45] Youngstrom DW, Rajpar I, Kaplan DL, Barrett JG. A bioreactor system for in vitro tendon differentiation and tendon tissue engineering. J Orthop Res 2015;33:911–8.
[46] Milet C, Duprez D. The Mkx homeoprotein promotes tenogenesis in stem cells and improves tendon repair. Ann Transl Med 2015;3:S33.